

Orientation dependence of high-order harmonic generation in molecules

M. Lein,^{1,*} P. P. Corso,² J. P. Marangos,¹ and P. L. Knight¹

¹*Blackett Laboratory, Imperial College of Science, Technology and Medicine, London SW7 2BW, United Kingdom*

²*Dipartimento di Scienze Fisiche ed Astronomiche dell'Università and Istituto Nazionale di Fisica della Materia, Via Archirafi 36, 90123 Palermo, Italy*

(Received 21 October 2002; published 28 February 2003)

We present two- and three-dimensional model calculations of high-order harmonic generation in H_2^+ . The harmonic spectra exhibit clear signatures of intramolecular interference. An interference minimum appears at a harmonic order that depends on the molecular orientation. Harmonic generation in three-center molecules is studied on the basis of two-dimensional calculations for a H_3^{2+} model system. From analytical considerations, the orientation dependence of the harmonic intensities in three-center molecules exhibits a double minimum due to intramolecular interference. In the numerical results, the double minimum is broadened into a single wide minimum. The effect of nonzero laser ellipticity on harmonic generation is investigated by means of two-dimensional simulations for H_2^+ . We find that harmonic generation with elliptical polarization is governed by interference effects similar to linear polarization.

DOI: 10.1103/PhysRevA.67.023819

PACS number(s): 42.65.Ky, 33.80.Rv

I. INTRODUCTION

High-order harmonic generation (HHG) [1–4] is the process in which a laser-driven system converts many incoming laser photons into a single high-energy photon. Using HHG as an efficient source of high-frequency coherent radiation is one of the main goals of research in this field [5–7]. HHG has been studied in many different systems, but most of the experimental and theoretical work has been focused on atoms.

The recollision picture [8,9] explains HHG as a sequence of tunnel ionization, laser-driven motion of the free electron, and recombination with the core. HHG with small molecules resembles HHG with atoms because the wave packet associated with a recolliding electron is typically much larger than the internuclear distance. However, since molecules have more degrees of freedom than atoms, their behavior in strong fields is richer and lends itself to targeted control by the experimenter. For example, HHG can be enhanced by pre-aligning the molecules in the interaction region [10,11]. Furthermore, some molecules tolerate unusually high laser intensities [12–14]. Therefore, one may hope that higher harmonic yields and higher photon energies can be reached with molecules.

Several earlier theoretical studies have shown that harmonic generation with linearly polarized light is sensitive to the molecular orientation [15–19]. The most dramatic orientation effect appears to be the interference between the contributions from the different atoms within the molecule [18,19], which can lead to a complete suppression of harmonics. The conditions for constructive and destructive interference were found to be rather simple and independent of the laser parameters. By varying the orientation of the molecule, a certain harmonic can be maximized or minimized. For diatomic molecules, it was found that the harmonic order

of an interference extremum depends only upon the projection of the internuclear separation onto the polarization axis.

The conclusions of Refs. [18,19] were largely based on two-dimensional (2D) model calculations for two-center molecules in linearly polarized lasers. In this paper, we compare those with the results of 3D calculations, which require a much larger amount of CPU time. We confirm from the comparison that the interference effects are independent of the dimensionality of the system. Furthermore, our analysis is extended to 2D calculations for three-center molecules. Here, we also find pronounced interference structures. The main motivation for the study of three-center systems is the experiment of Refs. [10,11] in which laser-induced alignment was demonstrated most clearly for CS_2 molecules. Finally, we investigate HHG in elliptically polarized lasers. Again, clear signatures of interference are found. However, the simple model of intramolecular interference given in Ref. [19] does not apply to elliptical polarization because the model implies that the impact velocity of recolliding electrons is parallel to the polarization axis. Accordingly, the interference pattern becomes more complicated for nonzero ellipticity.

This paper is organized as follows. Section II describes our numerical method. Sec. III gives a comparison between 2D and 3D results for H_2^+ . In Sec. IV, we report on the 2D treatment of the three-center system H_3^{2+} . Section V describes HHG with elliptical laser polarization, based on 2D calculations for H_2^+ . Finally, Sec. VI contains a short summary and our conclusions.

II. METHOD

In our numerical approach, we solve the time-dependent Schrödinger equation for a molecule in a strong laser pulse with electric field $\mathbf{E}(t)$,

$$i\frac{\partial}{\partial t}\Psi(\mathbf{r},t)=\left(\frac{\mathbf{p}^2}{2}+\mathbf{p}\cdot\mathbf{A}(t)+V(\mathbf{r})\right)\Psi(\mathbf{r},t), \quad (1)$$

*Present address: Max Planck Institute for the Physics of Complex Systems, Nöthnitzer Strasse 38, D-01187 Dresden, Germany.

where $\mathbf{A}(t) = -\int_0^t \mathbf{E}(t') dt'$, and $V(\mathbf{r})$ is the binding potential. The interaction between molecule and laser is treated in the dipole approximation. The nuclei are kept fixed during the action of the pulse.

In two dimensions, we first consider a model H_2^+ molecular ion. For this system, the solution of the Schrödinger equation and the calculation of the harmonic spectra follows closely the description in Ref. [18], involving a two-center soft-core Coulomb potential of the form

$$V(\mathbf{r}) = -\sum_{j=1,2} \frac{1}{\sqrt{\epsilon + \mathbf{r}_j^2}}, \quad (2)$$

where $\mathbf{r}_j = \mathbf{r} - \mathbf{R}_j$ with \mathbf{R}_1 and \mathbf{R}_2 being the positions of the nuclei. With the softening parameter $\epsilon = 0.5$, we reproduce the electronic ground-state energy of real H_2^+ (-30 eV).

As an example of a three-center molecule, we study the model H_3^{2+} molecular ion that has been described in Ref. [17]:

$$V(\mathbf{r}) = -\sum_{j=1}^3 \frac{1}{\sqrt{\epsilon + \mathbf{r}_j^2}}. \quad (3)$$

It differs from the H_2^+ model system merely by adding one potential well at \mathbf{R}_3 so that all three nuclei are situated along a straight line and form an inversion symmetric molecule with 2 a.u. distance between adjacent nuclei. The ground-state energy of this system is -41 eV. The central potential well is deeper than the outer ones, although the nuclear charge is the same for all three sites. This is because the central potential well is lowered by the presence of two neighboring wells.

In a three-dimensional treatment of H_2^+ , one would ideally integrate the Schrödinger equation using the full two-center Coulomb potential with its two singularities. This has been achieved for the special case of linear polarization with the H_2^+ molecular ion aligned parallel to the field [20]. When the molecular axis is not parallel to the field, the situation is truly three-dimensional and thus much more complicated. To simplify the numerical propagation, we do not use the bare Coulomb potential but a smooth two-center potential. In contrast to soft-core potentials applicable in 1D and 2D, we cannot use the functional form of Eq. (2) if the system is to reproduce the ionization potential of a real H_2^+ molecular ion. This is simply because any nonvanishing softening parameter $\epsilon > 0$ in Eq. (2) creates a potential that is above the bare Coulomb potential ($\epsilon = 0$) for all coordinates \mathbf{r} , thereby giving rise to a ground-state energy level above the ground state of real H_2^+ . Instead, we choose a two-center potential of the form

$$V(\mathbf{r}) = -\sum_{j=1,2} \frac{1}{\sqrt{\kappa + \mathbf{r}_j^4 / (\mathbf{r}_j^2 + \eta)}}. \quad (4)$$

For $\eta = 0$, the potential Eq. (4) assumes the functional form of the standard soft-core potential. For $\kappa = \eta = 0$, we retrieve the bare Coulomb potential. With the choice $\eta = 0.28$ and

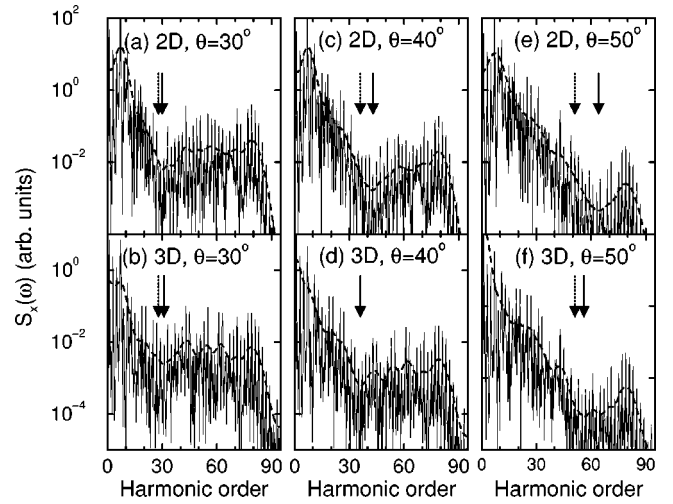


FIG. 1. Spectra of harmonics polarized parallel to the laser field for various orientations of H_2^+ in a 780-nm pulse with 5×10^{14} W/cm² intensity. (a),(c),(e) 2D calculation. (b),(d),(f) 3D calculation. Dashed curves, smoothed spectra; solid arrows, numerical positions of the interference minima; dashed arrows, positions of the interference minima as predicted by Eq. (5).

$\kappa = 0.1$, the H_2^+ electronic ground-state energy of -30 eV is reproduced at the internuclear distance $R = 2$ a.u. These softening parameters are relatively small as compared to $\epsilon = 0.5$ in the 2D calculations. This means that the 3D potential has deep wells (-3.7 a.u. minimum value), and we expect that our 3D analysis gives a reasonable approximation of the strong-field dynamics in the bare 3D Coulomb potential.

In all cases, the time-dependent Schrödinger equation, Eq. (1) is solved numerically by means of the split-operator method [21]. The harmonic spectra are calculated by Fourier transformation of the time-dependent dipole-acceleration expectation value [22]. The 3D calculations are very time-consuming and therefore restricted to linear polarization and a relatively small grid. We use a grid size of $276 \times 57 \times 51$ a.u., which is sufficient to calculate converged harmonic spectra. Here, 276 a.u. is for the direction parallel to the electric field, and 57 a.u. is for the direction perpendicular to the field and within the plane spanned by molecule and field. In the 2D calculations, we work with a grid of 368×68 a.u. for linearly polarized laser pulses and 368×368 a.u. for elliptical polarization.

Unless stated otherwise, we use 10-cycle laser pulses of 780 nm wavelength and 5×10^{14} W/cm² intensity. The electric-field envelope is trapezoidal with a three-cycle turn on and turn off.

III. COMPARISON OF 2D AND 3D RESULTS

In Fig. 1 we compare the results of 2D and 3D calculations for H_2^+ at the equilibrium internuclear distance $R = 2$ a.u. Shown are the spectra of harmonics polarized parallel to the laser field for three different molecular orientations: $\theta = 30^\circ$, $\theta = 40^\circ$, and $\theta = 50^\circ$, where θ is the angle between molecular axis and field. These angles were chosen

because they give rise to interference minima in the plateau region of the harmonic spectrum. The figure shows that although the fine details of the 2D and 3D spectra differ, they exhibit the same interference effect: a broad minimum is found in all spectra, which shifts towards higher harmonic orders with increasing angle of alignment. The suppression is due to destructive interference between the contributions from the two atomic centers. It was shown in Ref. [19] that the position of the minimum is approximately given by the simple relation

$$R \cos \theta = \lambda/2, \quad (5)$$

where $\lambda = 2\pi/k$ is the de Broglie wavelength of a recolliding electron that gives rise to the emission of a harmonic photon with frequency $\omega = k^2/2$. The 3D spectra are more structured, making it harder to localize the position of the interference minimum. We determine its position after applying a smoothing procedure to the spectra,

$$S_{\text{smooth}}(\omega) = \int S(\tilde{\omega}) \exp[-(\tilde{\omega} - \omega)^2/\sigma^2] d\tilde{\omega}, \quad (6)$$

where $\sigma = 3\omega_L$ with ω_L being the laser frequency. This procedure yields the dashed curves in Fig. 1. From the figure we find that the interference minimum (the deepest local minimum in the plateau region) for $\theta = 30^\circ$ is at the 30th (31st) harmonic order in 2D (3D). For $\theta = 40^\circ$, it is located at the 43rd (36th) order, and for $\theta = 50^\circ$, it is located at the 64th (56th) order. These values agree reasonably well with Eq. (5) which predicts orders of 28, 36, and 51, respectively. The arrows in Fig. 1 indicate the numerical positions of the interference minima as well as the predictions of Eq. (5). Apparently, the 3D results agree better with Eq. (5). This is probably due to the deeper potential wells making the process of harmonic generation more similar to the emission from two point sources. The latter was assumed in the derivation of Eq. (5). Nevertheless, we conclude that the 2D calculations yield a good description of the intramolecular interference effects.

In Fig. 2 we show the total harmonic spectra. These are obtained by adding the spectra of harmonics polarized parallel and perpendicular to the laser field. Although the perpendicular component is weak, it obscures the presence of the interference minimum. In particular, the interference minimum has essentially disappeared in the 3D spectra for the smaller alignment angles $\theta = 30^\circ$ and $\theta = 40^\circ$.

At the single-molecule level, the total harmonic intensities are the sum of the intensities polarized parallel and perpendicular to the field. However, this is not necessarily true in an experiment with many molecules aligned along the same direction. Here, the laser propagation has to be taken into account as well. Consider the following two cases.

(i) If the laser propagation direction is within the plane spanned by the molecular axis and the electric field, the perpendicular component of the induced dipole will point along the propagation axis. Hence, this component will not give rise to any emission into the propagation direction. Emission

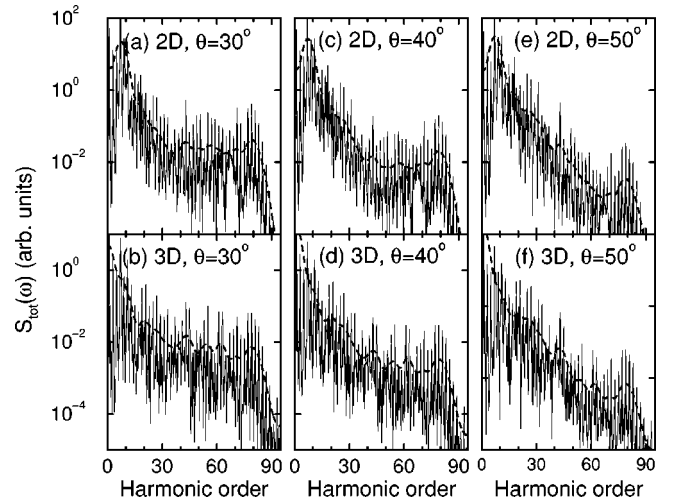


FIG. 2. Total harmonic spectra for various orientations of H_2^+ in a 780-nm pulse with $5 \times 10^{14} \text{ W/cm}^2$ intensity. (a),(c),(e) 2D calculation. (b),(d),(f) 3D calculation. Dashed curves; smoothed spectra.

into any other direction is impossible due to the lack of phase matching. Then, essentially only the parallel component is measured (Fig. 1).

(ii) On the other hand, if the propagation direction is perpendicular to the plane spanned by molecule and field, the perpendicular component can radiate into the propagation direction where it will be phase matched. In this case, the spectrum that one measures is the sum of both polarizations (Fig. 2).

Experimentally, it should be possible to make use of case (i) to suppress the perpendicular component so that a clearer interference structure is obtained.

IV. THE H_3^{2+} MODEL MOLECULE

We now turn our attention to a different problem: harmonic generation in three-center molecules. In our H_3^{2+} model system, we have not only an additional atomic site acting as an emitter of harmonics. Also, the three sites are nonequivalent as explained in Sec. II. Therefore, we expect more complicated interference patterns.

Figure 3 shows the total harmonic spectra calculated for 2D H_3^{2+} with an internuclear distance of $R = 2$ a.u. between two adjacent nuclei. Although these are the total harmonic spectra, we can clearly observe a rather broad interference minimum moving towards higher harmonic orders with increasing angle between molecule and field. Eventually, the minimum moves beyond the cutoff so that the plateau is essentially monotonously decreasing at $\theta = 60^\circ$.

To obtain a clearer picture of the interference effect, we turn to the orientation dependence of selected harmonics. This is shown in Fig. 4 for the 41st harmonic (left panel) and 71st harmonic (right panel). For most angles, the harmonics polarized perpendicular to the laser are relatively weak. Therefore, the orientation dependence of the total yield closely follows the parallel component. The perpendicular component exhibits a minimum around the same angle as the

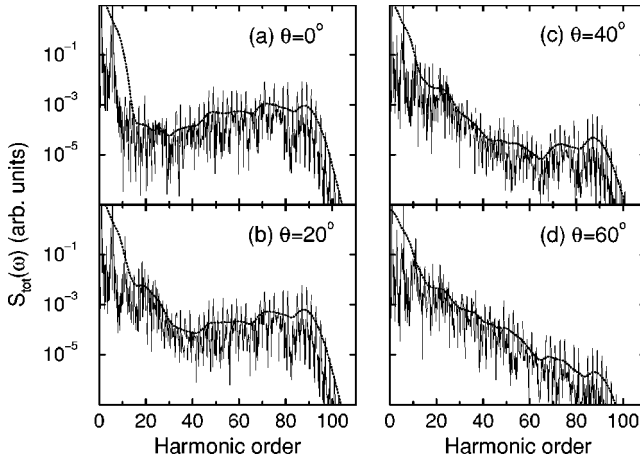


FIG. 3. Harmonic spectra for various orientations of 2D H_3^{2+} with internuclear distance $R=2$ a.u. between adjacent nuclei. Dashed curves, smoothed spectra.

parallel component. This is in contrast to two-center molecules, where local minima of the perpendicular component occur only at $\theta=0^\circ$ and $\theta=90^\circ$ [18]. For both polarizations, the interference minimum is rather broad and not as deep as previously found for two-center molecules. Actually, it seems to consist of two minima, which are smeared out to form a single broad minimum. For example, the 71st harmonic is slightly suppressed at $\theta=40^\circ$ in addition to the minimum at $\theta=60^\circ$. To investigate this point, we apply a crude model of point emitters situated at the positions of the nuclei. (This is analogous to the model used in Ref. [19] for diatomic molecules.) We then expect that the amplitude for harmonic emission due to recollision of an electron with wave-vector \mathbf{k} is proportional to an interference term describing the different phases of the electron wave at the positions \mathbf{R}_j of the nuclei,

$$A^{(3)} \sim \sum_{j=1}^3 \psi_0(\mathbf{R}_j) e^{i\mathbf{k} \cdot \mathbf{R}_j}, \quad (7)$$

where $\psi_0(\mathbf{r})$ is the ground-state wave function. With $\mathbf{R}_1 = -\mathbf{R}$, $\mathbf{R}_2 = 0$, $\mathbf{R}_3 = \mathbf{R}$, and $|\mathbf{R}| = R$, the amplitude in Eq. (7) gives rise to a harmonic intensity proportional to

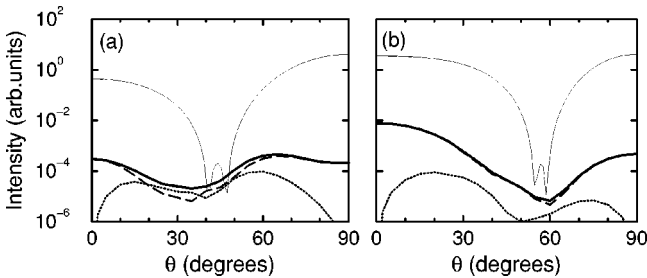


FIG. 4. Orientation dependence of the harmonic yield in H_3^{2+} for the 41st harmonic (left) and the 71st harmonic (right). Shown is the total signal (thick solid lines) which is the sum of the parallel component (dashed lines) and the perpendicular component (dotted lines). The thin upper lines show the prediction of Eq. (8).

$$|A^{(3)}|^2 \sim 1 + 4\gamma \cos(kR \cos \theta) + 4\gamma^2 \cos^2(kR \cos \theta), \quad (8)$$

with $\gamma = \psi_0(\mathbf{R})/\psi_0(0)$. The predictions of Eq. (8) are shown as the upper (thin solid) curves in Fig. 4. Indeed, for both the 41st and 71st harmonic we find a double minimum. Its location is in good agreement with the numerical results for the 71st harmonic, but the agreement is only modest for the 41st harmonic. Furthermore, the separation between the two minima within the double minimum is smaller than the width of the broad minimum obtained numerically. It seems that for a quantitative description of the three-center interference with nonequivalent atomic sites, the detailed shape of the binding potential has to be taken into account.

Although our analytical considerations indicate that the number of atoms in the molecule determines the number of interference minima, the numerical results show that it is difficult to deduce the number of atoms from the harmonic spectra. Diatomic molecules can produce spectra very similar to those in Fig. 3 if the internuclear distance is chosen appropriately.

V. ELLIPTICAL POLARIZATION

To study the influence of ellipticity on HHG in molecules, we return to the 2D H_2^+ model molecule. We consider an electric field of the form

$$\mathbf{E}(t) = E_0(t) [\mathbf{e}_x \sin(\omega t) + \mathbf{e}_y \xi \cos(\omega t)], \quad (9)$$

where ξ is the laser ellipticity. In the 2D simulation we are restricted to the situation where the molecular axis lies within the laser polarization plane.

For a linearly polarized laser, the harmonic spectrum is invariant under rotation of the molecular axis around the polarization axis, i.e., it depends only on the angle θ between molecule and field. For elliptical polarization, there is no such symmetry. Similarly, the spectrum depends on whether the laser polarization is left handed or right handed. The consequence for the 2D model is that for a given ellipticity, the harmonic spectrum changes when the molecule is reflected about the x axis. In our simulation, we therefore vary the orientation of the molecule from $\theta = -90^\circ$ to $\theta = 90^\circ$. In Fig. 5 we compare the orientation dependence of the 31st and 61st harmonic for three different ellipticities, $\xi=0$, $\xi=0.3$, and $\xi=0.5$. As expected, the harmonic yield drops very fast with increasing ellipticity because the recolliding electron “misses” the core when the polarization is not linear. The higher the ellipticity, the smaller is the overlap of the recolliding electron wave packet with the molecular core.

For $\xi=0$, the spectrum is symmetric around $\theta=0$, and we observe the familiar deep interference minima in the orientation dependence of the harmonics polarized parallel to the field. The y component is zero at $\theta=0$ and $\theta=\pm 90^\circ$ for symmetry reasons.

For nonzero ellipticity, the orientation dependence becomes asymmetric as explained above. The interference minima remain, but their positions change with ellipticity. In some cases, additional minima appear. These changes do not

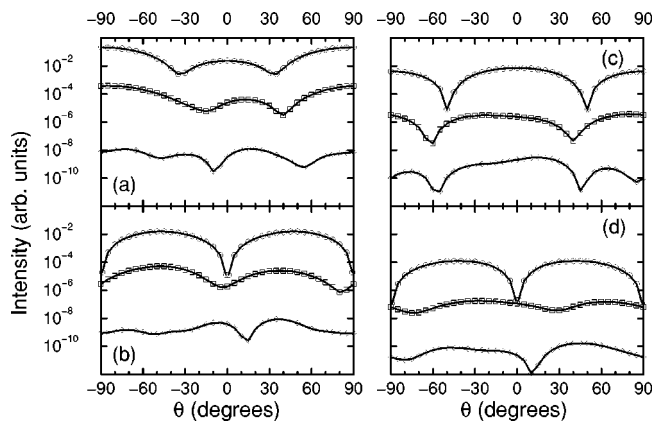


FIG. 5. Orientation dependence of the 31st harmonic (left-hand side) and the 61st harmonic (right-hand side) in 2D H_2^+ for the laser ellipticities $\xi=0$ (circles), $\xi=0.3$ (squares), and $\xi=0.5$ (diamonds). (a),(c) 31st and 61st harmonic polarized parallel to the larger component of the field. (b),(d) 31st and 61st harmonic polarized perpendicular to the larger component of the field. The calculation was performed for \sin^2 -shaped 8-cycle pulses of 5×10^{14} W/cm 2 intensity.

seem to follow any simple rules. For $\xi=0$ and $\xi=0.3$, the x component is large when θ is close to 0° or $\pm 90^\circ$, whereas the y component becomes large at intermediate values of θ . This general rule breaks down for $\xi=0.5$. In all cases, however, the harmonics are very sensitive to the molecular orientation: the typical variation is about two orders of magnitude.

An important conclusion is that HHG with any type of polarization can be greatly enhanced when aligned molecules are used instead of randomly oriented molecules. The optimal angle of alignment depends on the ellipticity. At present, we cannot make a quantitative comparison between fixed alignment and random orientation. This would require calculations for all molecular orientations, including the case that the molecular axis is not in the plane of polarization. Such 3D simulations of HHG in elliptically polarized laser pulses are currently out of reach.

VI. CONCLUSIONS

We have analyzed HHG in molecules with a focus on the interference between the different atomic sites. We have first compared 2D and 3D calculations for H_2^+ . While the detailed structure of the spectra depends on the number of dimensions, we found that the structures due to intramolecular interference are very similar. The harmonic spectra exhibit an interference minimum, which moves to higher harmonic orders with increasing angle between molecule and field.

The same interference effect is encountered in three-center molecules as shown in 2D calculations on a H_3^{2+} model system. The interference minimum in three-center systems, however, is actually a broadened double minimum.

For elliptical laser polarization, the interference effects persist, but the conditions for constructive and destructive interference deviate from the simple rules found for linear laser polarization.

In all cases, the harmonic yield is very sensitive to the molecular orientation, indicating that harmonic generation can be greatly enhanced if aligned molecules are used instead of randomly oriented molecules.

In our calculations, the nuclei were fixed. Thereby, the effect of the vibrational motion was neglected. Yet, it is expected that the interference structures remain intact if the laser-pulse duration is shorter than the vibrational period. Then, the harmonic spectrum serves as a snapshot of the molecular geometry. Experimentally, this seems possible for virtually any molecule since pulse lengths of less than 10 fs are available today. For a first experimental demonstration of the interference effect, however, H_2^+ will clearly be less appropriate than a heavier molecule with slower nuclear motion.

ACKNOWLEDGMENTS

This work was supported by the U.K. Engineering and Physical Sciences Research Council and by the European Union IHP Program (Grant No. HPRN-CT-1999-00129).

- [1] A. McPherson *et al.*, J. Opt. Soc. Am. B **4**, 595 (1987).
- [2] A. L'Huillier, K.J. Schafer, and K.C. Kulander, J. Phys. B **24**, 3315 (1991).
- [3] M. Protopapas, C.H. Keitel, and P.L. Knight, Phys. Rep. **60**, 389 (1997).
- [4] P. Salières, A. L'Huillier, P. Antoine, and M. Lewenstein, Adv. At., Mol., Opt. Phys. **41**, 83 (1999).
- [5] T. Ditmire, J.K. Crane, H. Nguyen, L.B. DaSilva, and M.D. Perry, Phys. Rev. A **51**, R902 (1995).
- [6] J.-F. Hergott *et al.*, Phys. Rev. A **66**, 021801(R) (2002).
- [7] E. Takahashi, Y. Nabekawa, T. Otsuka, M. Obara, and K. Midorikawa, Phys. Rev. A **66**, 021802(R) (2002).
- [8] P.B. Corkum, Phys. Rev. Lett. **71**, 1994 (1993).
- [9] K.C. Kulander, J. Cooper, and K.J. Schafer, Phys. Rev. A **51**, 561 (1995).
- [10] R. Velotta, N. Hay, M.B. Mason, M. Castillejo, and J.P. Marangos, Phys. Rev. Lett. **87**, 183901 (2001).
- [11] N. Hay *et al.*, Phys. Rev. A **65**, 053805 (2002).
- [12] A. Talebpour, C.-Y. Chien, and S.L. Chin, J. Phys. B **29**, L677 (1996).
- [13] C. Guo, M. Li, J.P. Nibarger, and G.N. Gibson, Phys. Rev. A **58**, R4271 (1998).
- [14] S.M. Hankin, D.M. Villeneuve, P.B. Corkum, and D.M. Rayner, Phys. Rev. Lett. **84**, 5082 (2000).
- [15] H. Yu and A.D. Bandrauk, J. Chem. Phys. **102**, 1257 (1995).
- [16] R. Kopold, W. Becker, and M. Kleber, Phys. Rev. A **58**, 4022 (1998).
- [17] D.G. Lappas and J.P. Marangos, J. Phys. B **33**, 4679 (2000).
- [18] M. Lein, N. Hay, R. Velotta, J.P. Marangos, and P.L. Knight, Phys. Rev. Lett. **88**, 183903 (2002).

- [19] M. Lein, N. Hay, R. Velotta, J.P. Marangos, and P.L. Knight, *Phys. Rev. A* **66**, 023805 (2002).
- [20] S. Chelkowski, T. Zuo, and A.D. Bandrauk, *Phys. Rev. A* **46**, R5342 (1992).
- [21] M.D. Feit, J.A. Fleck, Jr., and A. Steiger, *J. Comput. Phys.* **47**, 412 (1982).
- [22] K. Burnett, V.C. Reed, J. Cooper, and P.L. Knight, *Phys. Rev. A* **45**, 3347 (1992).